ORGANIC LETTERS

2012
Vol. 14, No. 8
1998–2001

# Dynamic Assembly of Porphyrin Wires Trapped on a Highly Oriented Pyrolitic Graphite Surface

**Vivien Rauch,[†] Jennifer A. Wytko,[†] Mayuko Takahashi,[‡] Yoshihiro Kikkawa,[*,‡] Masatoshi Kanesato,[‡] and Jean Weiss[*,†]**

*CLAC, Institut de Chimie, UMR 7177 CNRS-UDS, BP 1032, 1 rue Blaise Pascal, 67070 Strasbourg, France, and National Institute of Advanced Industrial Science and Technology (AIST), 1-1-1 Higashi, Tsukuba, Ibaraki 305-8562, Japan*

*jweiss@unistra.fr; y.kikkawa@aist.go.jp*

**Received February 27, 2012**

## ABSTRACT

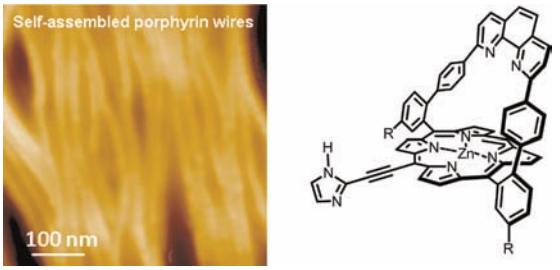


**Carefully designed porphyrin building blocks assemble through selective imidazole binding in various solvents to form linear multiporphyrin objects. From a dynamic mixture of monomers, dimers, and oligomers, linear objects were observed on a highly oriented pyrolitic graphite (HOPG) surface. On the surface, the objects' morphology clearly depended on the solvent used for deposition and was modified upon heating.**

Geometrically controlled self-assembly of molecular building blocks into nanostructures offers great potential for the design of nanomaterials due to the potential ease of processing for their integration in devices, especially in the form of molecular wires.[1] Among candidates as photo- or electroactive building blocks, tetrapyrrolic macrocycles in general, and porphyrins in particular, are especially attractive.[2] As a result, many aspects of porphyrin self-assemblies have been investigated over the past decade.[3] In general, self-assembly offers two tremendous advantages, which are a simplified synthetic approach and an increased availability of the building blocks. Noncovalent assembly has been successfully used, especially with stacked tetrapyrrolic macrocycles that form J-aggregates.[4] Such aggregation is a natural tendency that can be reinforced by electrostatic interactions[5] or tuned by solvent[6] and/or thermal[7] conditions. Both the exocyclic coordination of metal templates[8] or the axial coordination to a central metal core[9] have also led to multiple self-organized assemblies of porphyrins.

We recently described the efficient formation of multiporphyrin wires using highly directed imidazole recognition

[†] CLAC.

[‡] National Institute of Advanced Industrial Science and Technology.

(1) Weiss, J.; Koepf, M.; Wytko, J. A. In *Supramolecular Chemistry: from Molecules to Nanomaterials*; Steed, J. W., Gale, P. A., Eds.; John Wiley & Sons Ltd.: Chichester, U.K., 2012; Vol. 5, pp 2115−2148.

(2) (a) Jurow, M.; Schuckman, A. E.; Batteas, J. D.; Drain, C. M. *Coord. Chem. Rev.* **2010**, *254*, 2297. (b) Mohnani, S.; Bonifazi, D. *Coord. Chem. Rev.* **2010**, *254*, 2342. (c) Elemans, J. A. A. W.; van Hameren, R.; Nolte, R. J. M.; Rowan, A. E. *Adv. Mater.* **2006**, *18*, 1251.

(3) (a) Beletskaya, I.; Tyurin, V. S.; Tsivadze, A. S.; Guilard, R.; Stern, C. *Chem. Rev.* **2009**, *109*, 1659. (b) Drain, C. M.; Varotto, A.; Radivojevic, I. *Chem. Rev.* **2009**, *109*, 1630.

(4) Ji, H.-X.; Hua, J.-S.; Wan, L.-J. *Chem. Commun.* **2008**, 2653.

(5) Yeats, A. L.; Schwab, A. D.; Massare, B.; Johnston, D. E.; Johnson, A. T.; de Paula, J. C.; Smith, W. F. *J. Phys. Chem. C* **2008**, *112*, 2170.

(6) For a tutorial review, see: Gomar-Nadal, E.; Puigmartí-Luis, J.; Amabilino, D. B. *Chem. Soc. Rev.* **2008**, *37*, 490.

(7) Marangoni, T.; Mezzasakama, S. A.; Llanes-Pallas, A.; Yoosaf, K.; Armaroli, N.; Bonifazi, D. *Langmuir* **2011**, *27*, 1513.

(8) Richeter, S.; Jeandon, C.; Gisselbrecht, J.-P.; Ruppert, R.; Callot, H. J. *Inorg. Chem.* **2007**, *46*, 10241.

(9) (a) Ogawa, K.; Kobuke, Y. *Angew. Chem., Int. Ed.* **2000**, *39*, 4070. (b) Satake, A.; Fujita, M.; Kurimoto, Y.; Kobuke, Y. *Chem. Commun.* **2009**, 1231. (c) Kuramochi, Y.; Sandanayaka, A. S. D.; Satake, A.; Araki, Y.; Ogawa, K.; Ito, O.; Kobuke, Y. *Chem.—Eur. J.* **2009**, *15*, 2317.

10.1021/ol300488y 
**Published on Web 03/30/2012**

in phenanthroline-strapped porphyrin scaffolds.[10,11] The general design of the self-complementary self-assembling building blocks represented in Figure 1 comprises a 2-imidazolyl group connected to a phenanthroline-strapped zinc porphyrin as a recognition unit. For compounds **3Zn** and **4Zn**, the nature of the assembly can be controlled by choosing the appropriate surface (Figure 1). A hydrophilic surface forced the entropy governed thermodynamic self-assembly of dimers until precipitation of clusters on the surface, whereas a hydrophobic surface trapped the building blocks that could further assemble into linear wires.

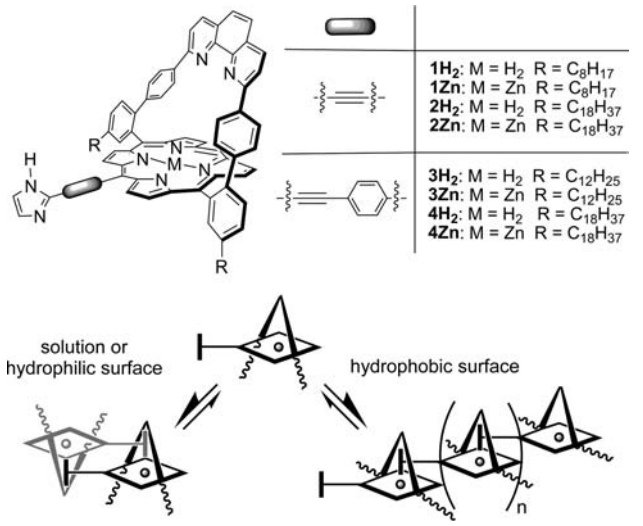


**Figure 1.** General structure of porphyrin-imidazole building blocks (top) and their two possible assembling modes (bottom).

This versatile behavior of the porphyrin monomers demonstrated that weak surface−molecule interactions can perturb an established assembly process in solution. Thus, we anticipated that small structural changes would favor the growth of porphyrin coordination polymers on the surface. Shorter alkyl side chains should increase the mobility of the species on the surface. The design, synthesis, and preliminary self-assembly properties on HOPG are described for two new monomers, **1Zn** and **2Zn** (Figure 1).

In these new phenanthroline-strapped porphyrin monomers, a short ethynyl, rather than a phenylethynyl moiety, bridges the imidazole and the porphyrin ring. Previous $^1$H NMR NOESY experiments on self-assembled dyads incorporating an ethynyl linker established that steric hindrance between the phenanthroline-strapped zinc porphyrin receptor and an imidazolyl-ethynyl porphyrin guest reduced its association constant.[12] Thus, we reasoned that if the association constant was lower, then surface−molecule interactions might predominate and consequently facilitate the surface-induced formation of longer linear oligomers. The $C_8$ and $C_{18}$ alkyl chains were chosen to provide different degrees of mobility to the **1Zn** and **2Zn** monomers on the deposition surface. As previously demonstrated, upon deposition on HOPG, compounds bearing long alkyl chains correspond to less mobile species[13] and, in the present work, should lead to shortened wires.

**Scheme 1**

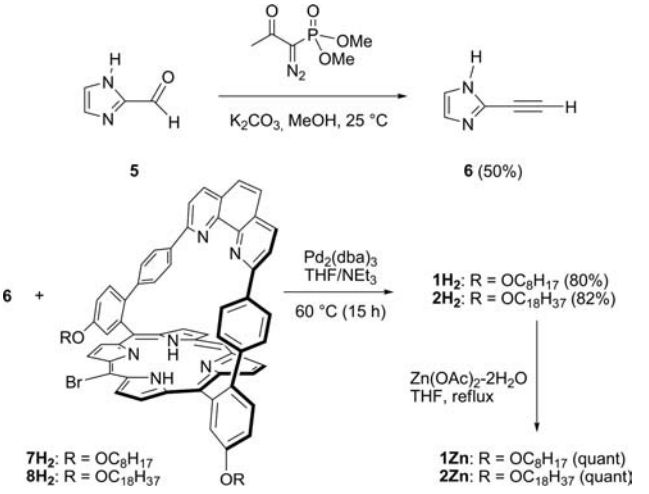


The 2-ethynylimidazole **6** was prepared by treating the commercially available aldehyde **5** with Bestman's reagent[14] to afford a 1/1 mixture of **6**[15] and starting material **5**, respectively (Scheme 1). Compound $\mathbf{7H_2}$ was synthesized in the same manner as previously reported for $\mathbf{8H_2}$.[10] Copper-free Sonogashira coupling[16] of unpurified **6** with $\mathbf{7H_2}$ or $\mathbf{8H_2}$ in the presence $Pd_2(dba)_3$ and $AsPh_3$ in a mixture of $NEt_3$/THF (3:7) at 60 °C for 1 h afforded the imidazolyl-ethynylporphyrins $\mathbf{1H_2}$ or $\mathbf{2H_2}$, respectively, in 80−85% yield.

The characterization of $\mathbf{1H_2}$ and $\mathbf{2H_2}$ was easily performed by conventional methods, whereas that of the corresponding self-associating zinc complexes **1Zn** and **2Zn** was significantly more difficult. After reaction of $\mathbf{1H_2}$ or $\mathbf{2H_2}$ in the presence of a large excess of zinc acetate, mass spectrometry confirmed the quantitative metalation

(10) Koepf, M.; Wytko, J. A.; Bucher, J. P.; Weiss, J. *J. Am. Chem. Soc.* **2008**, *130*, 9994.

(11) Koepf, M.; Conradt, J.; Szmytkowski, J.; Wytko, J. A.; Allouche, L.; Kalt, H.; Balaban, T. S.; Weiss, J. *Inorg. Chem.* **2011**, *50*, 6073.

(12) Paul, D.; Wytko, J.; Koepf, M.; Weiss, J. *Inorg. Chem.* **2002**, *41*, 3699.

(13) (a) Bléger, D.; Kreher, D.; Mathevet, F.; Attias, A.-J.; Arfaoui, I.; Metgé, G.; Douillard, L.; Fiorini-Debuisschert, C.; Charra, F. *Angew. Chem., Int. Ed.* **2008**, *47*, 8412. (b) Groszek, A. J. *Proc. R. Soc. London, Ser. A* **1970**, *314*, 473. (c) Qiu, X.; Wang, C.; Yin, S.; Zeng, Q.; Xu, B.; Bai, C. *J. Phys. Chem. B* **2000**, *104*, 3570. (d) Wang, H.; Wang, C.; Zeng, Q.; Xu, S.; Yin, S.; Xu, B.; Bai, C. *Surf. Interface Anal.* **2001**, *32*, 266 and references cited. (e) Venkataraman, B.; Breen, J. J.; Flynn, G. W. *J. Phys. Chem.* **1995**, *99*, 6608.

(14) Roth, G. J.; Liepold, B.; Muller, S. G.; Bestmann, H. J. *Synthesis* **2004**, *1*, 59.

(15) Codsford, N. D.; Kamenencka, T.; Roppe, J. R. U.S. Patent 20050085523, 2005.

(16) Wagner, R. E.; Johnson, T. E.; Li, F.; Lindsey, J. S. *J. Org. Chem.* **1995**, *60*, 635.

of the porphyrin nuclei of **1Zn** and **2Zn**. However, their $^1$H NMR spectra in $CDCl_3$ showed broad signals, as seen in Figure 2 for **2Zn**. These ill-defined spectra were attributed to the presence of multiple species in dynamic exchange. A very complicated spectrum was obtained at 298 K in $C_2D_2Cl_4$ and variable temperature (VT) experiments indicated a dynamic mixture of species (see Supporting Information), precluding any peak assignment.

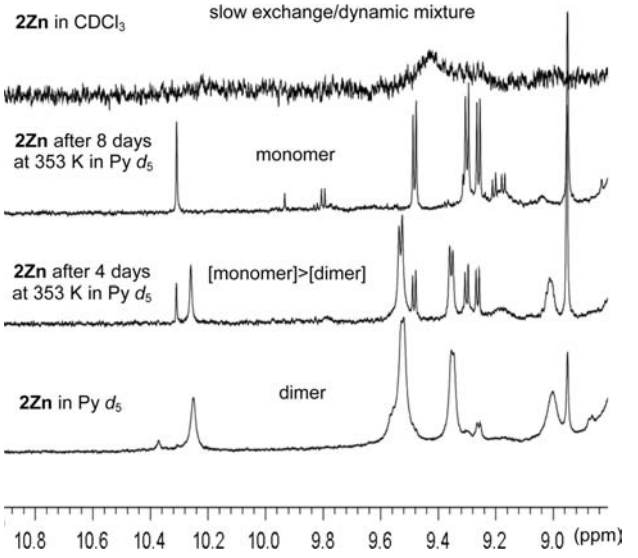


**Figure 2.** Comparison of $^1$H NMR spectra of **2Zn** in a noncoordinating (top) or strongly coordinating solvent. (The rest of the spectra are less informative due to the presence of pyridine peaks. Full spectra and VT experiments are provided in the Supporting Information.)

To destabilize assembled species and favor monomeric species, $^1$H NMR spectra were recorded in pyridine-$d_5$ for **1Zn**. In the initial NMR experiment, one species was observed in pyridine-$d_5$; however, after the sample was heated at 353 K for 4 days and cooled to 298 K, a second set of peaks appeared (Figure 2). Heating a sample at 353 K for 8 days afforded the spectrum of an isolated species of the **1Zn** monomer, most probably bound to the solvent. These features emphasize the extremely slow kinetics of exchange between the oligomer, dimer, and monomer in noncoordinating solvents.

Several DOSY NMR experiments were recorded for **1Zn** in pyridine-$d_5$ at different stages of heating (see Supporting Information) and at different concentrations. Before **1Zn** was heated in pyridine-$d_5$, the single species observed has a hydrodynamic radius of 3379 Å$^3$. After **1Zn** was heated at 353 K for 8 days, another single species, with a smaller hydrodynamic radius of 1730 Å$^3$, was detected in the solution. This smaller species was considered to be the monomer, possibly with a pyridine coordinated to the zinc center. DOSY experiments were tried in $C_2D_4Cl_4$ to estimate the size of the species in the dynamic mixture in a noncoordinating solvent. Unfortunately, these experiments were unsuccessful due to the poor resolution of the spectrum, which was similar to that obtained in $CDCl_3$ (see Figure 2).

Thus, a short ethynyl linker between the imidazole and the porphyrin renders the association of two building blocks *via* imidazole binding on the zinc less selective for the formation of dimeric species. This is consistent with the steric repulsion upon binding of the imidazole within the phenanthroline strap of a second molecule. In contrast, for the longer phenylethynyl linkers, the association equilibrium in aprotic solvents involves exclusively monomeric and dimeric species.[10,11] In the present case, the difficulties encountered in the characterization of a single species in a chlorinated solution seemed encouraging, as it strongly suggested that ill-defined larger species, which were different than soluble dimers, were formed.

The initial goal was to decrease the dimer association to increase the role of the surface during deposition of compounds **1Zn** and **2Zn**. Preliminary AFM imaging experiments suggested the presence of assembled linear species in solution prior to deposition on a surface. HOPG was selected as a substrate for deposition because it was used previously for surface-induced formation of oligomeric species.[10] In addition, HOPG is fully appropriate for developing interactions with the side chains of **1Zn** and **2Zn**. A first set of studies quickly indicated that in concentrated solutions random aggregation strongly competed with organized self-assembly (Supporting Information). Our attention then focused on less inert solvents, and Figure 3 summarizes several AFM experiments performed using weakly and strongly coordinating solvents.

A first set of experiments was performed by drop-casting micromolar THF solutions of **1Zn** and **2Zn** onto HOPG. The very short linear species observed (Figure 3a and d) were identified as objects formed in solution, given the inertness of the assemblies in solvents other than pyridine as indicated by NMR experiments. The heights of the objects (2.7 ± 0.5 nm) are more consistent with the presence of two linear species[17] on top of each other. In that case, the linear oligomers forming the top layer must come from an association that also takes place in solution. Their length can be shorter due to solubility limitations during the drop-casting of the solution onto the surface, and thus only partial overlap is seen (brightest contrast in Figure 3a and d). This behavior is almost identical to that observed in noncoordinating solvents such as $CHCl_3$ (see Supporting Information). In both cases, the objects observed on the HOPG surface correspond to a distribution of oligomers trapped by the interactions of alkyl chains with the lipophilic HOPG surface. Based on the mobility of the alkyl-substituted porphyrins on HOPG, the expected growth of the drop-casted objects was observed for both $C_8$ and $C_{18}$ after annealing at 60 °C (see Supporting Information). All other experiments were performed with $10^{-3}$ M monomer solutions that were obtained after

(17) The height of a monomer, from the porphyrin ring to the top of the phenanthroline strap, was estimated to be 1.25 nm based on molecular modeling.[10]

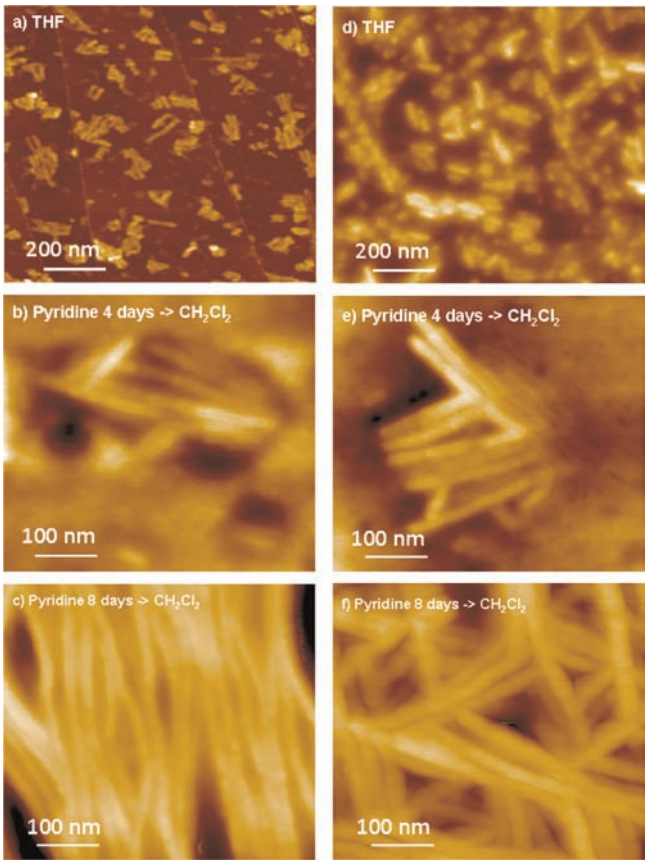


**Figure 3.** AFM images of solutions drop-casted on HOPG. Left (a–c): $C_8$ (**1Zn**); right (d–f): $C_{18}$ (**2Zn**); (a, d): THF solutions; (b, e): refluxed in pyridine for 4 days (b, e) or 8 days (c, f) then diluted to 10 $\mu$M in $CH_2Cl_2$.

refluxing in pyridine for 4–8 days. These solutions were then diluted (10 $\mu$M) in a given solvent to allow the system to slowly evolve again toward oligomeric species.

The presence of the bulky coordinating pyridine on the unhindered side of the zinc porphyrin, which is the side meant to develop interactions with the surface, controls the formation of coordination oligomers. The coordination of pyridine to the zinc atom is weaker than that of imidazole;[18] thus solvent evaporation facilitates the assembly process. The evolution of the dilute solution deposited on the surface was followed over time by AFM imaging. Only short molecular tapes (100–300 nm), but longer than those observed from $CHCl_3$ and THF, were formed from the pyridine solution that was heated for 4 days. With the NMR data taken into account, this solution could be a mixture of monomers and dimers, although monomeric forms should be highly favored at low concentrations ($> 10^{-6}$ M). However, heating in pyridine for 8 days enhanced the dissociation to monomers, and the slow self-assembly from the monomer state allowed the growth of longer molecular wires (600–900 nm), which are elongated from small droplets. These droplets, formed during the dewetting on the surface, possibly consist of amorphous monomer aggregates (see Supporting Information). Although the width of the objects appears different for **1Zn** and **2Zn** (Figure 3c and f) conclusions cannot be drawn about the morphology of each assembly because of the broadening effect of the AFM tip. However, it would be expected that $C_{18}$ side chains promote the bundling of individual wires to a larger extent than $C_8$ side chains. In any case, the shorter alkyl chains seemed to generate the longer objects. This observation is in agreement with previous reports.[10] These linear objects are among the straightest reported for an assembly process based on a single coordination bond and a hydrogen bond.

In conclusion, shortening the spacer between the porphyrin ring and the imidazole significantly perturbs the initially entropy-governed assembly process in solution. Conduction measurements after transfer to a dielectric surface are in progress as well as detailed thermodynamic and kinetic studies to determine the best solvent conditions for the formation of linear porphyrin arrays.

**Acknowledgment.** This work was supported by the CNRS and Université de Strasbourg. V.R. thanks the French Ministry of Research for his PhD financial support (MENRT). Y.K. thanks MEXT KAKENHI (23106722), Japan for financial support.

**Supporting Information Available.** Synthetic and experimental procedures, VT NMR spectra of **2Zn**, DOSY NMR of **1Zn**, cross-sectional data, additional AFM height, phase images and concentration effects. This material is available free of charge via the Internet at http://pubs.acs.org.

(18) Brandel, J.; Trabolsi, A.; Traboulsi, H.; Melin, F.; Koepf, M.; Wytko, J. A.; Elhabiri, M.; Weiss, J.; Albrecht-Gary, A.-M. *Inorg. Chem.* **2009**, *48*, 3743.

The authors declare no competing financial interest.